DOI: 10.1002/ejoc.201201629

Organic Chromophores Based on a Fused Bis-Thiazole Core and Their Application in Dye-Sensitized Solar Cells

Alessio Dessì,[a] Gabriella Barozzino Consiglio,[a] Massimo Calamante,[a] Gianna Reginato,*[a] Alessandro Mordini,[a] Maurizio Peruzzini,[a] Maurizio Taddei,[a,b] Adalgisa Sinicropi,[b] Maria Laura Parisi,[b] Fabrizia Fabrizi de Biani,[b] Riccardo Basosi,[b] Riccardo Mori,[c] Michele Spatola,[c] Mara Bruzzi,[c] and Lorenzo Zani*[d]

Keywords: Synthetic methods / Dyes/pigments / Fused-ring systems / Photochemistry / Sensitizers / Solar cells

Four new D-π-A organic dyes incorporating either a thiazolo[5,4-*d*]thiazole bicyclic system (**TTZ1**–**2**) or a benzo[1,2-*d*:4,5-*d*′]bisthiazole tricyclic unit (**BBZ1**–**2**) have been synthesized and fully characterized. The key steps of the synthesis include an efficient MW-assisted preparation of the thiazolo[5,4-*d*]thiazole core and selective functionalization of two different dihalothienyl derivatives through Suzuki coupling. All the compounds showed photo- and electrochemical properties compatible with their employment in dye-sensitized solar cells. In addition, their electronic structure and transitions were investigated by means of TD-DFT calculations. Dye-sensitized solar cells fabricated with dye **TTZ1** yielded an average power conversion efficiency corresponding to 43 and 60 % of the performances recorded under the same conditions for cells containing reference dyes **N3** and **D5**, respectively. Efficiency measurements and electrochemical impedance spectroscopy (EIS) experiments indicated that use of chenodeoxycholic acid (CDCA) as a co-adsorbent was beneficial to disrupt dye-dye interactions and slow down recombination processes within the cells, thus allowing power conversion efficiencies up to 3.53 % to be obtained.

Introduction

In the last decades, global energy demand has increased at a fast pace.[1] Presently, the world's growing energy needs are mostly satisfied by employment of fossil fuels, however, the resulting economic and environmental concerns are stimulating intense research in the field of renewable energy sources.[2] Among these, solar energy has often been described as the most promising option.[3] Silicon-based photovoltaic cells were the first devices capable of converting solar radiation into electricity; nowadays, they are a mature and reliable technology, but they still present some drawbacks, such as an expensive and energetically demanding production process and the requirement for highly pure starting materials.[4]

Since their appearance in 1991,[5] dye-sensitized solar cells (DSSCs) have been considered a potential low-cost and efficient alternative to traditional silicon-based photovoltaic devices.[6] In DSSCs, light harvesting is carried out by a photosensitizer absorbed on a thin layer of a mesoporous semiconductor (usually TiO_2); the photoexcited sensitizer transfers an electron to the semiconductor, thus achieving charge separation. Therefore, effective light absorption by the sensitizer is essential to obtain highly-efficient DSSCs.

Until recently, the most efficient DSSCs described in the literature incorporated polypyridyl complexes of Ru^{II} as the sensitizers,[7] which allowed power conversion efficiencies exceeding 11 % to be reached.[8] Despite this, ruthenium-based dyes still suffer from some important drawbacks, such as difficult purification procedures, low molar extinction coefficients and high cost of the metal precursors; such disadvantages prompted the search for alternative photosensitizers. Organic dyes[9] offer the possibility of overcoming many of the problems associated with the use of ruthenium-containing sensitizers; they can often be prepared from inexpensive starting materials using simple procedures and have high molar extinction coefficients. Furthermore, their stereoelectronic properties can be easily tuned by employing a flexible synthetic strategy. Not surprisingly, the development of new organic compounds to be used as sen-

[a] CNR – Istituto di Chimica dei Composti Organometallici (CNR-ICCOM),
Via Madonna del Piano 10, 50019 Sesto Fiorentino, Italy
Fax: +39-055-5225203
E-mail: gianna.reginato@iccom.cnr.it
Homepage: www.iccom.cnr.it
[b] Dipartimento di Biotecnologie, Chimica e Farmacia, Università degli Studi di Siena,
Via A. Moro 2, 53100 Siena, Italy
[c] Dipartimento di Ingegneria Industriale, Università degli Studi di Firenze,
Via S. Marta 3, 50139 Florence, Italy
[d] CNR – Istituto per la Sintesi Organica e la Fotoreattività (CNR – ISOF),
Via Piero Gobetti 101, 40129 Bologna, Italy
Fax: +39-051-6398349
E-mail: lorenzo.zani@isof.cnr.it
Supporting information for this article is available on the WWW under http://dx.doi.org/10.1002/ejoc.201201629.

 WILEY ONLINE LIBRARY © 2013 Wiley-VCH Verlag GmbH & Co. KGaA, Weinheim

sitizers in DSSCs has become a very active field of research.[10] Such compounds are usually characterized by a D-π-A architecture, in which a donor group (D) is connected to an acceptor/anchoring group (A) through a conjugated bridge (π). Upon irradiation, such an arrangement facilitates the generation of photoinduced intramolecular charge-transfer states, thus promoting electron injection into the nanocrystalline semiconductor.

Thiazolo[5,4-*d*]thiazoles **1** are a class of heterocyclic compounds endowed with a rigid and coplanar bicyclic scaffold giving rise to a highly extended π-electron system (Figure 1). The first compound of this class was prepared in 1891 by Ephraim,[11] but its correct structure was established only in 1960 by Johnson et al.,[12] who were the first to prepare a large number of analogues.[12,13] Thiazolo[5,4-*d*]thiazoles were initially investigated for their potential biological activity,[14] but later they were especially used as spacer units in semiconducting organic materials for polymer light-emitting diodes (PLEDs)[15] and organic field-effect transistors (OFETs).[16] More recently, the thiazolothiazole unit has been incorporated in donor/acceptor polymers used as the photoactive components of organic bulk heterojunction (BHJ) solar cells.[17] In particular, thiazolothiazole-containing polymers showed remarkable charge carrier diffusion lengths,[17e,17g,17h] and power conversion efficiencies as high as 5.8% were achieved.[18]

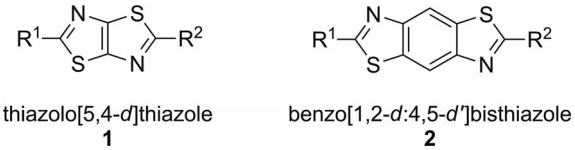

Figure 1. The thiazolo[5,4-*d*]thiazole (**1**) and benzo[1,2-*d*:4,5-*d*′]-bisthiazole (**2**) ring systems.

Benzo[1,2-*d*:4,5-*d*′]bisthiazoles **2** feature another interesting fused heterocyclic system, in which π-conjugation is further extended by the presence of an additional aromatic ring (Figure 1). Although the synthesis of these compounds was claimed in 1903,[19] subsequent studies proved the corresponding structural assignment to be incorrect and described alternative procedures with which to obtain the products with the correct regiochemistry.[20,21] In analogy with thiazolothiazoles, benzo[1,2-*d*:4,5-*d*′]bisthiazoles have also been extensively investigated for their applications in nonlinear optics[22] and organic (opto)electronics.[23] Further reports focused on their employment as fluorescent probes,[24] near-IR chromophores,[25] and liquid crystal precursors.[26] Moreover, they have recently been incorporated in photoactive polymers used in BHJ solar cells, reaching a maximum power conversion efficiency of 3.0%.[27]

Despite the large body of work outlined above, to the best of our knowledge the employment of thiazolo[5,4-*d*]-thiazoles and benzo[1,2-*d*:4,5-*d*′]bisthiazoles as photosensitizers for DSSCs has not yet been described. Therefore, we decided to prepare new organic dyes containing these two heterocyclic systems as spacer units and to assess their potential as DSSC sensitizers, with the goal of determining whether their interesting properties could also prove useful for such an application.

To this end, we designed compounds **TTZ1**–**2** and **BBZ1**–**2** (Figure 2). The well-characterized triarylamine and cyanoacrylate groups were selected as the donor and acceptor/anchoring moieties, respectively. Thiophene rings were placed next to the central heterocyclic core to extend the overall conjugation of the molecule. Finally, long alkyl chains were introduced on the thiophene rings to improve the solubility of the compound and to suppress dye aggregation on the semiconductor surface, as previously reported.[28]

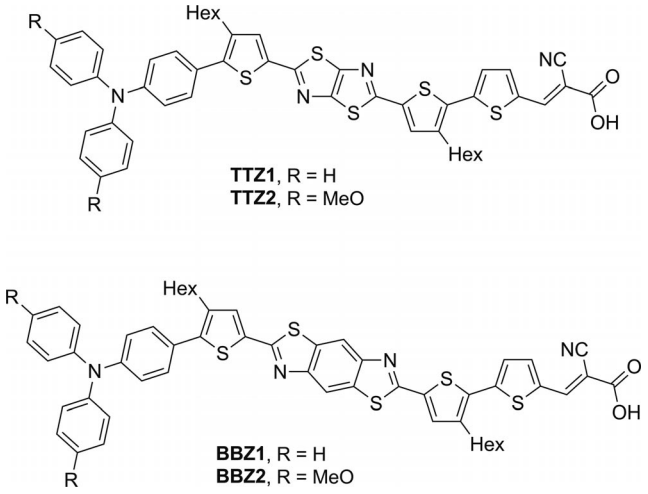

Figure 2. Sensitizers **TTZ1**–**2** and **BBZ1**–**2** synthesized in this work.

Herein, we report the synthesis of the new compounds, as well as their experimental and computational characterization. Furthermore, we present the results of efficiency measurements carried out on photovoltaic devices built using **TTZ1**–**2** and **BBZ1**–**2** as the light-harvesting materials.

Results and Discussion

Synthesis of the New Organic Sensitizers

Compounds **TTZ1**–**2** were prepared according to the synthetic sequence shown in Scheme 1. Treatment of 3-hexylthiophene with lithium 2,2,6,6-tetramethylpiperidide, generated in situ from *tert*-butyllithium and 2,2,6,6-tetramethylpiperidine, and quenching of the resulting thienyllithium species with *N*,*N*-dimethylformamide (DMF) afforded 4-hexylthiophene-2-carbaldehyde (**3**) as a single regioisomer. Interestingly, the same transformation using *n*BuLi as the base gave, instead, the product as a mixture of 2,4- and 2,3-regioisomers. Compound **3** was then reacted in the presence of dithiooxamide (**4**) to provide thiazolothiazole **5**. The reaction was performed under solvent-free conditions at 180 °C with microwave heating, giving the desired product in good yield.

 © 2013 Wiley-VCH Verlag GmbH & Co. KGaA, Weinheim

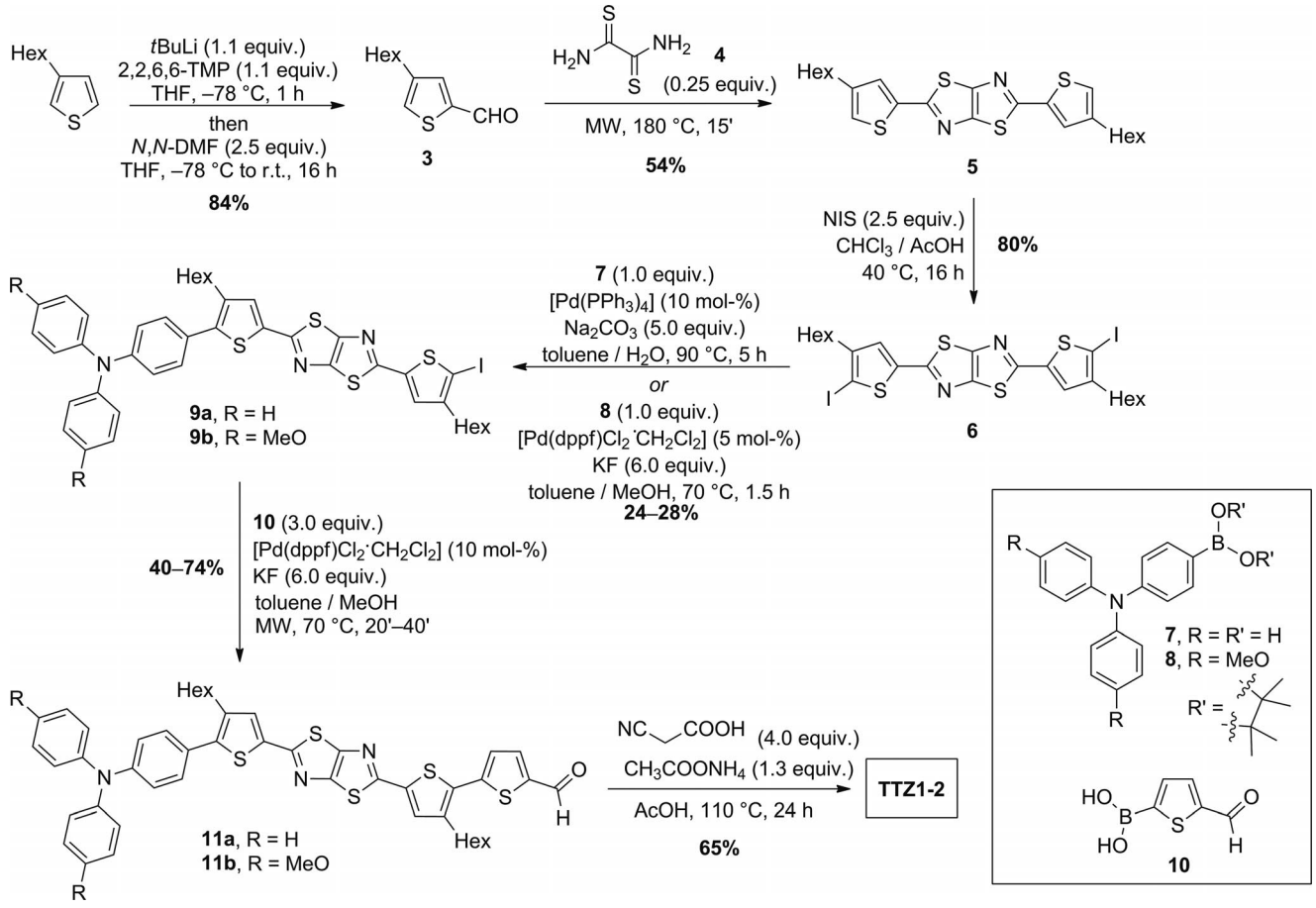

Scheme 1. Synthetic sequence employed for the preparation of sensitizers **TTZ1**–**2**.

It should be pointed out that this is the first microwave-assisted synthesis of a thiazolo[5,4-*d*]thiazole heterocycle reported to date. Indeed, all previous preparations employed conventional heating and most of them either used a large excess of aldehyde or were carried out in high-boiling solvents.[12–18,29] Using the conditions described above, we were able to both reduce reaction time and improve product yield compared with the previous methodology.[15] Unfortunately, use of an excess amount of aldehyde was still required, but the latter could be recovered during product purification by means of flash column chromatography and reused for the synthesis of compound **5**.

Iodination of heterocycle **5** by treatment with *N*-iodosuccinimide (NIS) at 40 °C overnight led to the formation of bis-iodo compound **6** in 80% yield. Compound **6** then underwent a Pd-catalyzed Suzuki coupling to introduce the triarylamine donor moiety. Two different organoboron compounds were employed for this transformation: commercially available 4-(diphenylamino)benzeneboronic acid (**7**) was used to prepare triphenylamino derivative **9a** (R = H), while boronic ester **8**, in turn obtained from the corresponding arylbromide,[30] was used for the synthesis of bis-methoxy-substituted analogue **9b** (R = MeO). In both cases, it was necessary to carefully monitor the reactions by TLC to ensure good conversion of the starting materials and, at the same time, minimize formation of the double coupled products. As a consequence, the reactions could not generally be driven to completion and provided products **9a**–**b** in only moderate yields (24–28%).

At this stage, a second Pd-catalyzed Suzuki coupling with 5-formyl-2-thiopheneboronic acid (**10**) was used to introduce a formyl group, leading to compounds **11a**–**b**. The latter transformation was found to proceed well when KF was employed as the base and heating was performed by microwave irradiation. Under these conditions the desired products could be obtained in moderate to good yields (40–74%) within short reaction times (20–40 min); use of different bases, such as sodium carbonate, and classical heating conditions, resulted in lower yields or longer reaction times. Finally, compounds **11a**–**b** were converted in good yields into sensitizers **TTZ1**–**2** by Knoevenagel condensation with excess cyanoacetic acid in the presence of ammonium acetate and glacial acetic acid as the solvent.[31]

The synthesis of compounds **BBZ1**–**2** was carried out in a similar manner, although some steps required slightly different conditions (Scheme 2). The starting material for the preparation of benzobisthiazole **13** was 2,5-diaminobenzene-1,4-dithiol bis-hydrochloride (**12**), which was treated with aldehyde **3** in DMF under thermal conditions. Unfortunately, microwave heating did not prove beneficial in this case. Electrophilic iodination of **13** with NIS proved to be extremely slow, and the starting material was not fully con-

 © 2013 Wiley-VCH Verlag GmbH & Co. KGaA, Weinheim

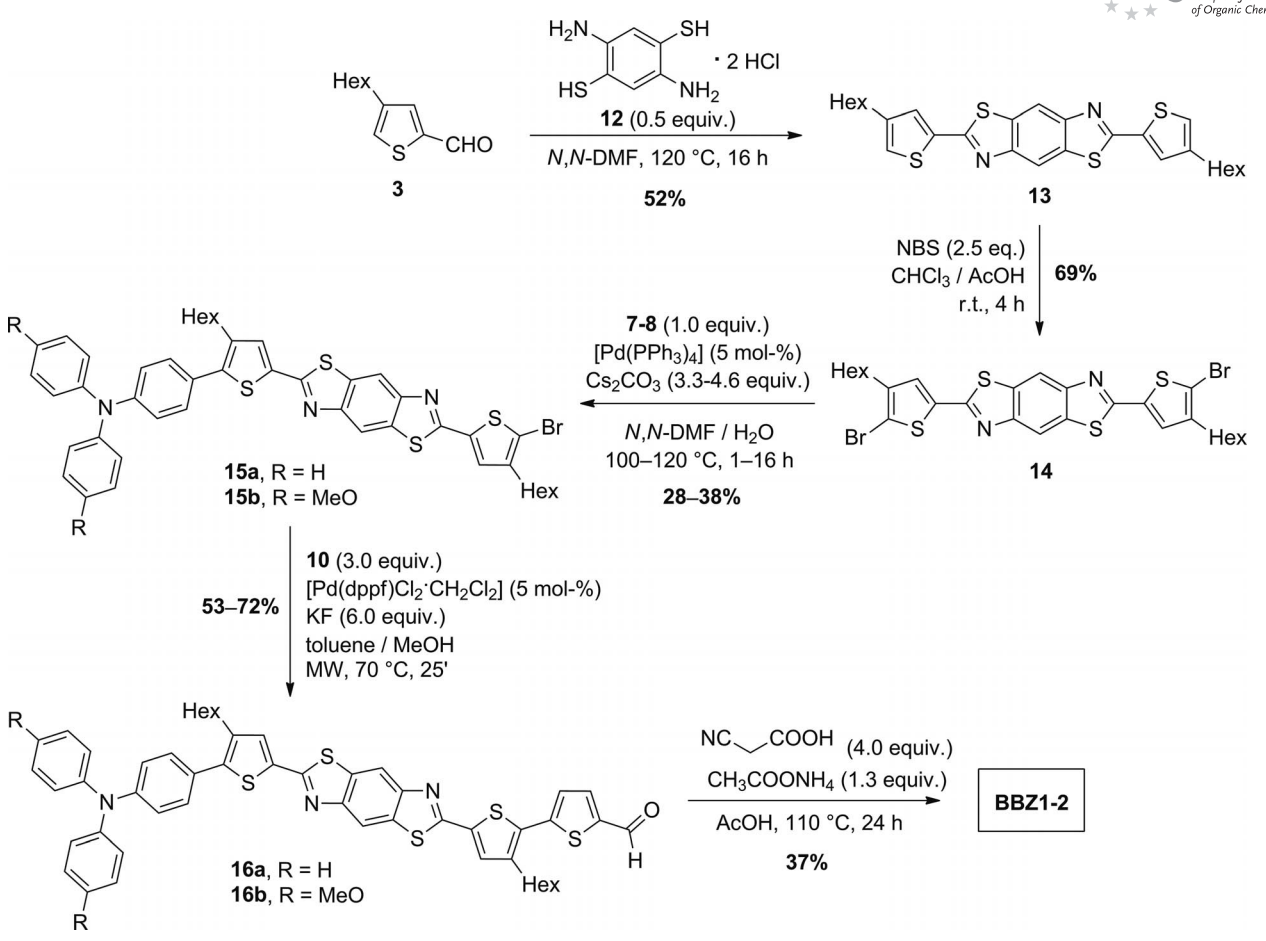

Scheme 2. Synthetic sequence employed for the preparation of sensitizers **BBZ1**–**2**.

verted even after a prolonged reaction time. For this reason, bis-bromo derivative **14** was prepared instead by reaction with *N*-bromosuccinimide (NBS), which required only four hours at room temperature. Bis-bromide **14** was then used as the key intermediate for the preparation of benzobisthiazoles **BBZ1**–**2**, which were obtained in moderate yields.

All the compounds were isolated in quantities large enough to allow full chemical characterization and fabrication of the corresponding photovoltaic devices. Compounds **TTZ1**–**2** and **BBZ1**–**2** were highly soluble in tetrahydrofuran (THF) but only moderately soluble in chlorinated solvents such as CH_2Cl_2 and $CHCl_3$, and almost completely insoluble in all other common organic solvents; therefore, TiO_2 sensitization proved possible only from THF solutions of the dyes (see the Exp. Section).

Optical Properties

The UV/Vis absorption spectra of compounds **TTZ1**–**2** and **BBZ1**–**2** in THF solution are displayed in Figure 3; the relevant optical data are summarized in Table 1. All compounds showed two main absorption bands: the absorption band at around 300 nm is probably due to a localized aromatic π–π* transition typical of the triarylamine fragment,[32] whereas the intense band found in the visible region can be attributed to a delocalized π–π* transition from the triarylamine and the central heterocyclic moiety to the cyanoacrylic function. These assignments are mainly based on the results of computational studies carried out on the sensitizers (see below). Thiazolothiazole species **TTZ1**–**2** showed a redshifted absorption compared with benzobisthiazole derivatives **BBZ1**–**2** (472–476 vs. 446–455 nm); the difference can be attributed to the presence of an additional aromatic ring in the latter structures, which stabilizes the HOMO–1 and HOMO orbitals relative to the LUMO, thus causing the observed hypsochromic shift. In addition, it can be observed that compounds **TTZ2** and **BBZ2**, featuring methoxy-substituted terminal benzene rings, had absorption maxima localized at slightly higher wavelengths compared with **TTZ1** and **BBZ1**. In this case, the discrepancy probably arises from the presence of electron-rich substituents on the triarylamine moiety, which increase its donor ability and cause the observed redshift. For all new sensitizers, the visible bands were characterized by good to high values of molar absorptivity ($\varepsilon = 2.76 \times 10^4$ $M^{-1}cm^{-1}$ for **TTZ1**; 4.36×10^4 for **TTZ2**; 3.64×10^4 for **BBZ1**; 6.32×10^4 for **BBZ2**). Such values are comparable to those of most organic sensitizers described to date, such as the well-known organic dye **D5**, which is reported to have $\varepsilon = 3.8 \times 10^4$ $M^{-1}cm^{-1}$ in CH_3CN solution.[33] Interestingly,

 © 2013 Wiley-VCH Verlag GmbH & Co. KGaA, Weinheim

Table 1. Optical and electrochemical properties of compounds **TTZ1–2** and **BBZ1–2**.

Cmpd	λ_{abs} ($\varepsilon \times 10^4$ M^{-1} cm^{-1}) [nm][a]	λ_{emi} [nm]	SS [cm^{-1}][b]	E_{0-0} [eV][c]	E_{ox} [V][d]	E^*_{ox} [V][d,e]
TTZ1	472 (2.76)	581	3975	2.33	1.14 (0.93)	–1.19
TTZ2	476 (4.36)	605	4479	2.31	0.93 (0.72)	–1.38
BBZ1	446 (3.64)	537	3780	2.51	1.15 (0.94)	–1.36
BBZ2	455 (6.32)	534	3251	2.46	0.92 (0.71)	–1.54

[a] UV/Vis spectra were recorded on a 2.5×10^{-5} M solution of the dye in THF. [b] Stokes Shift. [c] Estimated from the intersection of the normalized absorption and emission spectra. [d] Potentials vs. NHE (potentials vs. Ag/AgCl NaCl 3 M are given in parentheses) measured in CH_2Cl_2 solution. [e] Calculated from $E_{ox} - E_{0-0}$.

benzobisthiazole derivatives **BBZ1–2** showed higher molar absorptivities compared with their thiazolothiazole analogues **TTZ1–2**. In addition, compounds containing methoxy-substituents absorbed light more intensely than compounds featuring simple phenyl rings. The UV/Vis spectrum of compound **TTZ1** on TiO_2 film features a broadened absorption band compared with that recorded in solution, with a slightly redshifted maximum (477 vs. 472 nm) and a more clearly redshifted onset (see the Supporting Information, Figure S1), suggesting a tendency to form *J*-aggregates on the semiconductor surface.[34]

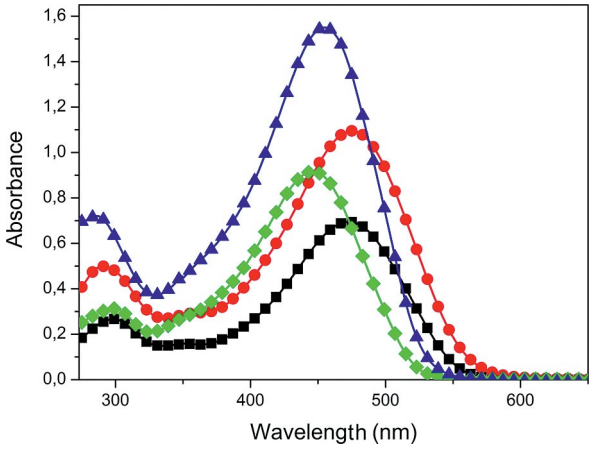

Figure 3. UV/Vis absorption spectra of compounds **TTZ1–2** and **BBZ1–2** in THF solution ($c = 2.5 \times 10^{-5}$ M). **TTZ1**: black squares; **TTZ2**: red circles; **BBZ1**: green rhombs; **BBZ2**: blue triangles.

Fluorescence emission spectra (Figure 4) were recorded by irradiating the samples at their maximum absorption wavelengths. Compounds **TTZ1–2** emitted at higher wavelengths compared with **BBZ1–2**, and were also characterized by larger Stokes shifts (Table 1). Thiazolothiazole **TTZ2** had both the most redshifted emission at 605 nm and the largest Stokes shift at 4479 cm^{-1}, suggesting the occurrence of an intramolecular charge transfer excitation process.[35]

From the intersection between the normalized absorption and emission spectra, the optical band gap of the novel sensitizers (corresponding to the zero-zero transition energy, E_{0-0}) was calculated. Thiazolothiazoles had much smaller optical band gaps compared with benzobisthiazoles, whereas the optical band gaps of triphenylamine species were slightly larger than those of methoxy-substituted compounds. The corresponding values are reported in Table 1.

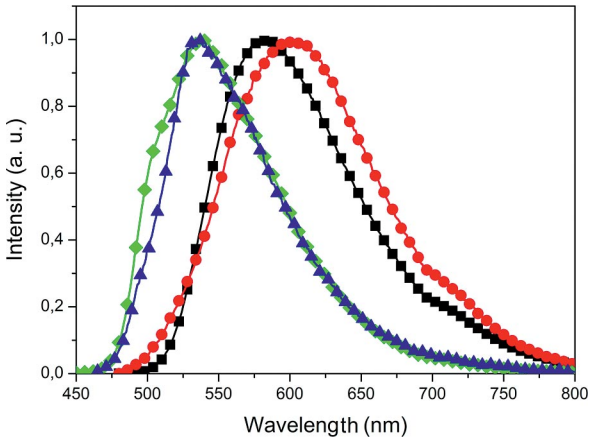

Figure 4. Normalized fluorescence emission spectra of compounds **TTZ1–2** and **BBZ1–2** in THF solution. **TTZ1**: black squares; **TTZ2**: red circles; **BBZ1**: green rhombs; **BBZ2**: blue triangles.

Electrochemical Measurements

The electrochemical characteristics of the new sensitizers were investigated by means of cyclic voltammetry (CV) in CH_2Cl_2 solution. The cyclic voltammogram of compound **TTZ1** is presented in Figure 5, while the relevant electrochemical data for all compounds are reported in Table 1 (for the cyclic voltammograms of compounds **TTZ2** and **BBZ1–2** see Figure S2). All dyes displayed a first oxidation

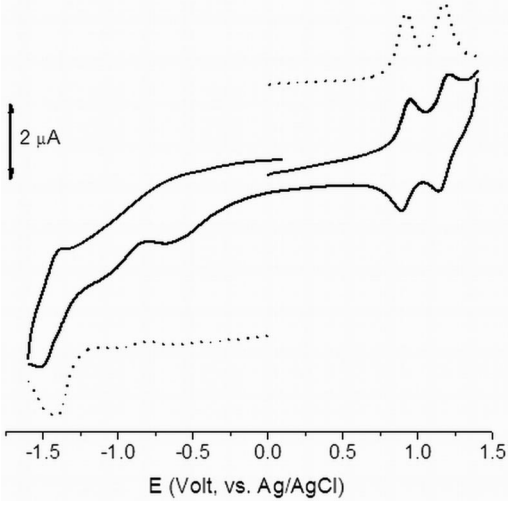

Figure 5. Cyclic voltammogram of compound **TTZ1** in CH_2Cl_2 solution.

 © 2013 Wiley-VCH Verlag GmbH & Co. KGaA, Weinheim

process (E_{ox}) in the 0.92–1.15 V range (vs. NHE), which can be attributed to removal of one electron from the triarylamine moiety. Indeed, methoxy-substituted dyes **TTZ2** and **BBZ2** showed less positive ground-state oxidation potentials than triphenylamine-bearing dyes **TTZ1** and **BBZ1** (0.92–0.93 V compared with 1.14–1.15 V, vs. NHE). Clearly, the presence of electron-rich methoxy-substituents on the donor group makes the corresponding compounds easier to oxidize than those lacking such functionalities. On the other hand, the presence of such substituents also affects the chemical reversibility of the redox process, as indicated by the i_{pc}/i_{pa} ratio measured at 0.2 Vs^{-1}, which decreases from 1 (for **TTZ1** and **BBZ1**) to 0.8 (for **TTZ2** and **BBZ2**).

The ground-state oxidation potentials of all the new compounds are more positive than that of the I^-/I_3^- redox couple (0.4 V vs. NHE), thus assuring dye regeneration during operation of a DSSC. Based on the experimental optical band gap values (2.31–2.51 eV), we calculated the excited state oxidation potential (E^*_{ox}) of the dyes to be between –1.54 and –1.19 V (vs. NHE; Table 1). Such values are sufficiently more negative than that of the conduction band of TiO_2 (–0.5 V) to guarantee electron injection from the dye to the semiconductor.

To further characterize the spectroscopic features and the redox behavior of the new compounds, spectroelectrochemical measurements were conducted by observing the UV/Vis spectral changes of all the compounds upon oxidation in CH_2Cl_2 solution; as an example, the spectra obtained for compound **TTZ1** are shown in Figure 6. As previously noted, the UV/Vis spectrum of this species shows two distinct bands, which, under these experimental conditions, are found at 300 and 486 nm and could be attributed to localized and delocalized aromatic π→π* transitions, respectively.[35] As shown in Figure 6, removal of the first electron from **TTZ1** causes a change in its absorption properties, resulting in a decrease of both these bands. At the same time, a broad band appears at lower energy (centered at 680 nm) and one isosbestic point is maintained at 550 nm, suggesting that **TTZ1**$^+$ radical cation is reasonably stable under these conditions. The appearance of this broad absorption has been previously observed[36,37] and has been assigned to the HOMO/(HOMO–1)→SOMO transitions in triarylamine radical cations, in agreement with our interpretation of **TTZ1** redox behavior. A similar behavior has also been observed for compounds **TTZ2** and **BBZ1**–**2**, with methoxy-substituted compounds having the new band appearing at lower energy compared with their triphenylamine counterparts.

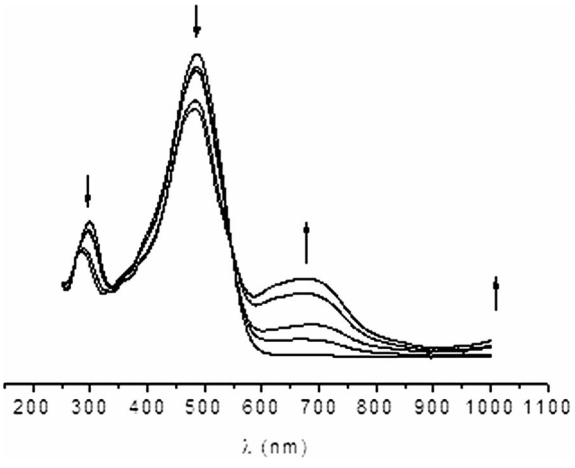

Figure 6. UV/Vis spectra recorded upon stepwise oxidation of **TTZ1** in a OTTLE cell in CH_2Cl_2 solution; supporting electrolyte: $[NBu_4][PF_6]$ (0.2 M).

Computational Analysis

The electronic structure of the new sensitizers was studied by means of density functional theory (DFT) calculations using the Gaussian 09 software package.[38] First, the ground-state geometries of compounds **TTZ1**–**2** and **BBZ1**–**2** were optimized in vacuo by using the B3LYP functional and the 6-31G* basis set. From such optimization, it became apparent that the dyes assume a largely planar structure along most of the conjugated system, with small dihedral angles between adjacent rings (<20°); in all compounds, the only substantial deviation from coplanarity was found at the thiophene-phenyl junction, where the two rings form a 47–48° dihedral angle for steric reasons (see Figure S3 in the Supporting Information).

The complete set of wave function plots for all the studied compounds is reported in Figure S4. From an inspection of the computed frontier orbital electron density distributions, we can conclude that, for all compounds, the HOMO–1 orbital is mainly located on the conjugated bridge, with a sizeable contribution coming from the terminal thiophene ring (see insets in Figure 7 and Figure S4); in the HOMO, the electron density is mainly found on the donor triarylamine group, whereas for the LUMO it is concentrated on the acceptor cyanoacrylic group. As far as orbital energies are concerned (Figure 7), our calculations indicate that the HOMO–1 (localized on the central heterocycle) is strongly stabilized moving from the thiazolothiazole- to benzobisthiazole-containing compounds, as a consequence of the increase in aromaticity due to the presence of the central benzene ring. Both the HOMO and the HOMO–1 are instead destabilized when methoxy-substituents are placed on the terminal phenyl ring. LUMO energies, on the other hand, are relatively unaffected by the changes in molecular structure. As a consequence, methoxy-substituted compounds **TTZ2** and **BBZ2** display reduced energy gaps, leading to slightly redshifted absorption maxima, whereas benzobisthiazoles **BBZ1**–**2** exhibit larger energy gaps than their thiazolothiazole counterparts **TTZ1**–**2**, leading to a blueshifted absorption.

The TD-CAM-B3LYP/6-31G* absorption maxima (λ^a_{max}), excitation energies (E_{exc}) and oscillator strengths (f) of dyes **TTZ1**–**2** and **BBZ1**–**2**, both in vacuo and in THF, are shown in Table 2.

For all dyes, the excitation process in the visible region is mainly due to the HOMO–1→LUMO transition, account-

 © 2013 Wiley-VCH Verlag GmbH & Co. KGaA, Weinheim

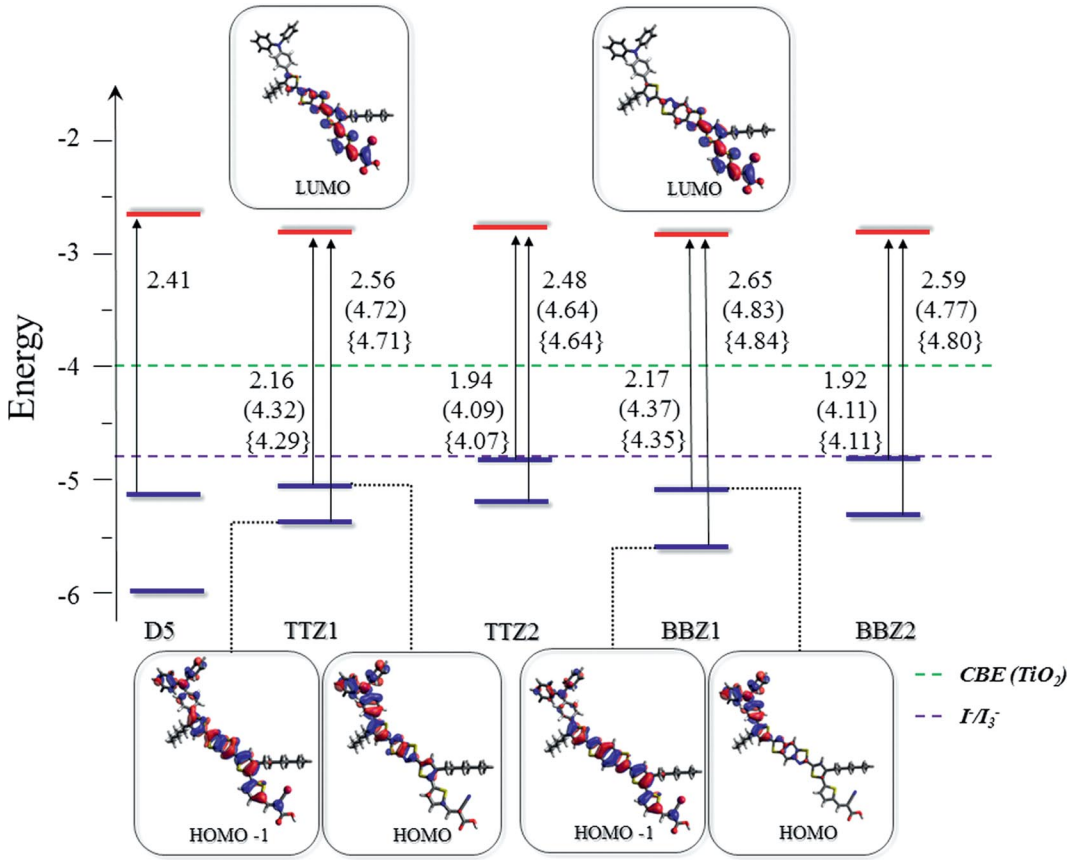

Figure 7. HOMO–1, HOMO and LUMO energies of compounds **TTZ1**–**2** and **BBZ1**–**2**; the values for **D5** are reported for comparison. Computed B3LYP and TD-CAM-B3LYP, both in vacuo (in parentheses) and in THF {in brace}, HOMO–LUMO (bottom left) and HOMO–1-LUMO (top right) energy differences (in eV) are shown next to vertical arrows. The conduction band edge (CBE) level of the TiO_2 (–4.0 eV) and the redox potential of the I^-/I_3^- couple (ca. –4.8 eV) are indicated by the dashed green and purple lines.[39] The wave function plots for compounds **TTZ1** and **BBZ1** are also shown.

Table 2. Experimental and TD-CAM-B3LYP computed absorption maxima (λ^a_{max}), excitation energies (E_{exc}) and oscillator strengths (f) for dyes **TTZ1**–**2** and **BBZ1**–**2** in vacuo and in THF.

	λ_{abs} [nm][a]	λ^a_{max} [nm]		E_{exc} [eV]	f
TTZ1	472	THF	466	2.66	2.35
		in vacuo	482	2.57	2.45
TTZ2	476	THF	470	2.64	2.39
		in vacuo	486	2.50	2.55
BBZ1	446	THF	437	2.83	2.42
		in vacuo	451	2.75	2.47
BBZ1	455	THF	440	2.82	2.50
		in vacuo	453	2.74	2.55

[a] UV/Vis spectra were recorded on a 2.5×10^{-5} M solution of the dye in THF.

ing for 51–68% of the total, whereas the HOMO→LUMO transition contributes only 9–29%, depending on the molecule studied. Both these transitions are productive in terms of electron injection because they transfer electron density from either the spacer or the donor group to the acceptor cyanoacrylic group, which is in closest proximity to the semiconductor surface. TD-DFT values are in good agreement with the experimental results with an error of at most 0.1 eV.

Photoelectrochemical Measurements

Once their characterization was complete, the new dyes were used for the fabrication of a series of test solar cells to verify their photovoltaic performances. It should be pointed out that the cells produced during this work were not fully optimized, for example by introducing a scattering titania layer or by adjusting the electrolyte composition. Indeed, our aim at this stage was to evaluate the potential of compounds **TTZ1**–**2** and **BBZ1**–**2** as dyes for DSSCs by comparing their performance with those of reference sensitizers, such as Ru complex **N3** and organic compound **D5**. The corresponding results are summarized in Table 3.

Initially, we prepared two series of cells by using dye **TTZ1** and a iodide/triiodide-based electrolyte, either in the absence or in the presence of the well-known co-adsorbent chenodeoxycholic acid (CDCA). The average efficiency of the cells built with **TTZ1** alone reached 43% of the performance yielded by a **N3**-containing cell[7] measured under the same conditions; it also corresponded to 60% of the efficiency observed for the standard organic dye **D5**.[33] In the case of organic dyes, co-adsorption with cholic acid derivatives has often been reported to improve the efficiency of the corresponding DSSCs, thanks to their tendency to

 © 2013 Wiley-VCH Verlag GmbH & Co. KGaA, Weinheim

Table 3. Photovoltaic parameters of DSSCs built using the new organic sensitizers as well as reference dyes **D5** and **N3**.[a]

Sensitizer	Additive	J_{sc} [mA cm^{-2}]	V_{oc} (mV)	*ff*	η [%]
TTZ1	–	5.48	0.583	0.72	2.56
TTZ1	CDCA	6.92	0.621	0.74	3.53
TTZ2	CDCA	5.24	0.591	0.73	2.53
BBZ1	CDCA	4.76	0.594	0.74	2.32
BBZ2	CDCA	3.76	0.564	0.71	1.67
D5	–	8.92	0.614	0.71	4.29
N3	–	11.80	0.639	0.71	5.93

[a] *J*-*V* curves measured under AM 1.5G simulated solar irradiation (90 mW cm^{-2}) at room temperature; film thickness approx. 10 μm; active area 0.25 cm^2.

disrupt unfavorable dye-dye interactions, thus facilitating electron injection.[40] We found that cells fabricated by using **TTZ1** in combination with CDCA showed improved photovoltaic parameters compared with those not containing the co-adsorbent (Table 3 and Figure 8), which resulted in a considerable increase of power conversion efficiency (η) from 2.56 to 3.53%. Based on the increase both in short-circuit current (J_{sc}) and open-circuit voltage (V_{oc}), we concluded that addition of CDCA was necessary to minimize detrimental dye-dye interactions and to hinder reverse electron transfer from the semiconductor to triiodide, thereby reducing the dark current. An analogous behavior has been previously observed by adding CDCA to DSSCs sensitized with compound **D5**.[41] Based on these results, CDCA was used in the fabrication of all the following photovoltaic devices.

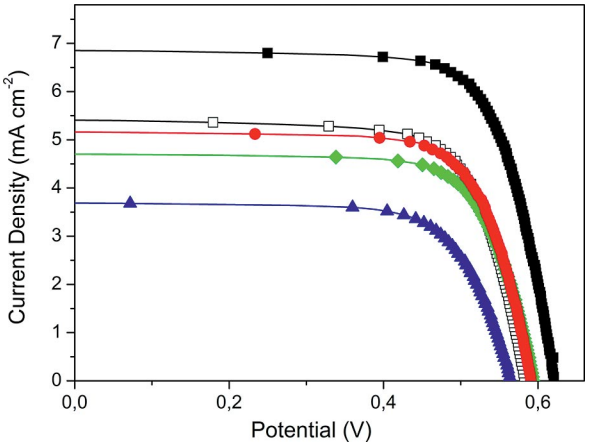

Figure 8. Representative current/voltage curves of DSSCs built using sensitizers **TTZ1**–**2** and **BBZ1**–**2**. **TTZ1**: hollow squares; **TTZ1**+CDCA: black squares; **TTZ2**+CDCA: red circles; **BBZ1**+CDCA: green rhombs; **BBZ2**+CDCA: blue triangles.

Unfortunately, the other photosensitizers investigated in this study provided inferior photovoltaic performance compared with dye **TTZ1**. Benzobisthiazole sensitizers **BBZ1**–**2** gave worse results than their thiazolothiazole counterparts (Table 3), yielding both lower photocurrent and photovoltage. The decrease in J_{sc} could be attributed to a less efficient adsorption of benzobisthiazole sensitizers on the semiconductor surface. To prove this point, we measured the density of adsorbed methoxy-containing dyes **TTZ2** and **BBZ2** on TiO_2, and found values of 4.0×10^{-7} and 2.9×10^{-7} mol cm^{-2}, respectively. Thus, the lower density of adsorbed benzobisthiazole dyes compared with thiazolothiazoles could at least in part explain the difference in the observed efficiencies. In addition, despite their superior light-harvesting properties, methoxy-substituted species **TTZ2** and **BBZ2** gave rise to less efficient photovoltaic cells in comparison with triphenylamine-containing dyes **TTZ1** and **BBZ1**. Possibly, the destabilization induced in the ground-state HOMO level by the methoxy substituents (see above) hindered dye regeneration by the electrolyte, thus leading to the observed decrease in photovoltaic performance.

The encouraging results described above suggest that the central thiazolothiazole core could find use as a spacer unit in efficient organic DSSC sensitizers, provided that further structural optimization is carried out on the dyes.

Electrochemical Impedance Spectroscopy

Understanding charge transfer processes taking place within a solar cell is crucial to explain the variation in photovoltaic performance of devices built under different conditions. Electrochemical impedance spectroscopy (EIS) is a powerful technique that allows the interfacial charge transfer and internal electron transport processes that occur during operation of a DSSC to be characterized.[42] We carried out measurements on cells built using the most effective sensitizers, namely thiazolothiazoles **TTZ1**–**2**, over the 100 kHz to 0.1 Hz frequency range in the dark at –0.6 V forward bias voltage; the resulting Nyquist plots are presented in Figure 9.

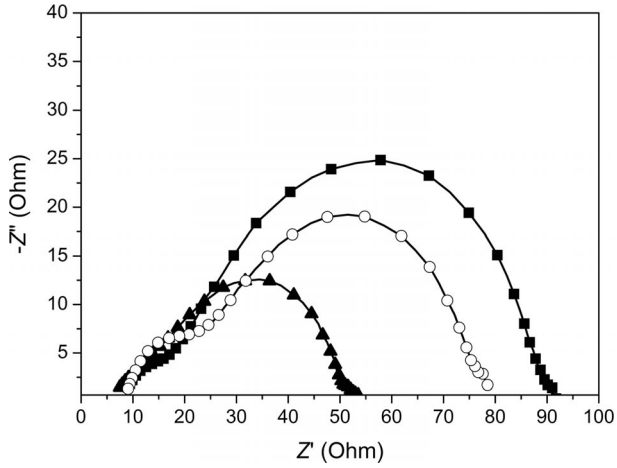

Figure 9. EIS plots of cells built using sensitizers **TTZ1**–**2**. **TTZ1**: black triangles; **TTZ1**+CDCA: black squares; **TTZ2**+CDCA: hollow circles.

In such plots, the large semicircle in the mid-frequency domain reflects the charge transfer resistance relative to both electron diffusion across the nanocrystalline titania layer and the electron recombination reaction between the semiconductor and the electrolyte at the sensitized-TiO_2/

 © 2013 Wiley-VCH Verlag GmbH & Co. KGaA, Weinheim

solution interface. As shown in Figure 9, the size of the semicircles decreases in the order **TTZ1**+CDCA > **TTZ2**+CDCA > **TTZ1**, which is in agreement with the order of the corresponding V_{oc} values reported in Table 3. In particular, the semicircle relative to the cell in which **TTZ1** was used in combination with CDCA is significantly larger than that corresponding to **TTZ1** alone. Such increase in diameter indicates a higher resistance to interfacial electron transfer from the conduction band of TiO_2 to triiodide in the electrolyte solution. This finding is in agreement with the different V_{oc} values obtained from the *J*/*V* curves (Figure 8), and confirms that adsorption of CDCA is useful to reduce the amount of dark current when sensitizer **TTZ1** is employed.

Conclusions

Four new photosensitizers, **TTZ1**–**2** and **BBZ1**–**2**, containing either a thiazolo[5,4-*d*]thiazole- or a benzo[1,2-*d*:4,5-*d*′]bisthiazole spacer, have been prepared and characterized. Their synthesis featured a novel and efficient MW-assisted preparation of the thiazolo[5,4-*d*]thiazole core as well as the double functionalization of two different dihalothienyl derivatives through Suzuki coupling. The new compounds displayed interesting photo- and electrochemical properties, which made them applicable for the construction of dye-sensitized solar cells. TD-DFT calculations were carried out to probe the electronic structure and transitions of the dyes, and suggested that visible absorption was mostly due to a HOMO–1 → LUMO transition. Dye-sensitized solar cells built with compounds **TTZ1**–**2** and **BBZ1**–**2** yielded power conversion efficiencies up to 3.53%; such values were promising but did not exceed the photovoltaic performance of reference organic dye **D5**. An increase in efficiency was observed for the cells when TiO_2 staining was conducted in the presence of chenodeoxycholic acid (CDCA), probably due to minimization of unfavorable dye···dye interactions and reduction of reverse electron transfer from the semiconductor to triiodide, as seen by *J*/*V* and EIS measurements. Despite their drawbacks, the straightforward synthesis presented for these molecules and their encouraging photophysical properties suggest that the thiazolothiazole nucleus can be employed as a new core structure in organic π-dyes for DSSCs. The preparation of new sensitizers, based on the introduction of more efficient and suitable donor and acceptor groups and on the reduction of molecular aggregation, is underway in our laboratories and will be reported in due course.

Experimental Section

General Synthetic Remarks: All reactions were performed under an inert nitrogen atmosphere in flame- or oven-dried apparatus using Schlenk techniques.[43] Microwave-assisted transformations were carried out with a CEM Discover Bench-Mate reactor at fixed temperature and variable power. THF was distilled from metallic sodium in the presence of benzophenone; toluene was distilled from metallic sodium, methanol was distilled from metallic magnesium in the presence of a catalytic amount of iodine, and CH_2Cl_2 was distilled from $CaCl_2$. 2,2,6,6-Tetramethylpiperidine (TMP) was purified by distillation over CaH_2 and kept over KOH under a nitrogen atmosphere. Acetonitrile, valeronitrile and *tert*-butylpyridine were distilled before use. DMF was stored under nitrogen over 4 Å molecular sieves. 4-Bromo-*N*,*N*′-bis(4-methoxyphenyl)aniline[30] was prepared according to a published procedure. All other chemicals employed were commercially available and used as received. Petroleum ether (PE) was the 40–60 °C boiling fraction. Thin-layer chromatography was carried out on aluminum-supported Merck 60 F254 plates; detection was achieved using UV light and by staining with either permanganate or molybdophosphoric acid solutions followed by heating. Flash column chromatography[44] was performed using Merck Kieselgel 60 (300–400 mesh) as the stationary phase. ^{1}H NMR spectra were recorded at 300 or 400 MHz, and ^{13}C NMR spectra were recorded at 75.5 or 100.6 MHz, respectively, with Bruker Avance or Varian Mercury series instruments. Chemical shifts were referenced to the residual solvent peak ($CHCl_3$: δ = 7.26 ppm for ^{1}H NMR and δ = 77.16 ppm for ^{13}C NMR; [D$_8$]THF: δ = 1.72 and 3.58 ppm for ^{1}H NMR, δ = 67.21 and 25.31 ppm for ^{13}C NMR). FTIR spectra were recorded with a Perkin–Elmer Spectrum BX instrument in the range 4000–400 cm^{-1} with a 2 cm^{-1} resolution. ESI-MS spectra were obtained by direct injection of the sample solution using a Thermo Scientific LCQ-FLEET instrument and are reported in the form *m*/*z*. HRMS spectra were measured with a Thermo Scientific LTQ Orbitrap (FT-MS) instrument. UV/Vis spectra were recorded with a Varian Cary 400 spectrometer, and fluorescence spectra were recorded with a Varian Eclipse instrument, irradiating the sample at the wavelength corresponding to maximum absorption in the UV spectrum.

Synthetic Procedures

2,5-Bis(4-hexylthiophen-2-yl)thiazolo[5,4-*d*]thiazole (5): In a microwave vial equipped with a magnetic stirrer were introduced dithiooxamide (**4**; 0.218 g, 1.82 mmol, 1.0 equiv.) and 4-hexylthiophene-2-carbaldehyde (**3**; 1.43 g, 7.26 mmol, 4.0 equiv.). The resulting mixture was heated under microwave irradiation at 180 °C for 15 min, after which it was allowed to cool to room temperature. TLC analysis (SiO_2; PE/Et_2O, 15:1) showed the presence of the desired compound; the reaction mixture was diluted with H_2O (15 mL) and CH_2Cl_2 (15 mL), and the layers were separated. The aqueous phase was extracted with CH_2Cl_2 (2 × 15 mL) and the combined organic layers were washed with water (30 mL) and brine (30 mL), and dried with Na_2SO_4. Removal of the solvent in vacuo afforded a dark thick oil, which was purified by flash column chromatography (SiO_2; PE/Et_2O, 22:1) to give **5** as a brown solid (0.461 g, 0.97 mmol, 54%). ^{1}H NMR (300 MHz, $CDCl_3$): δ = 7.40 (d, *J* = 1.2 Hz, 2 H), 7.04 (d, *J* = 1.2 Hz, 2 H), 2.62 (t, *J* = 7.5 Hz, 4 H), 1.56–1.72 (m, 4 H), 1.25–1.43 (m, 12 H), 0.87–0.92 (m, 6 H) ppm. ^{13}C NMR (75 MHz, $CDCl_3$): δ = 162.8, 149.8, 144.6, 137.2, 128.2, 123.6, 31.8, 30.5, 30.4, 29.1, 22.7, 14.2 ppm. The data are in agreement with those reported in the literature.[15]

2,5-Bis(4-hexyl-5-iodothiophen-2-yl)thiazolo[5,4-*d*]thiazole (6): In a Schlenk flask equipped with a magnetic stirrer were introduced 2,5-bis(4-hexylthiophen-2-yl)thiazolo[5,4-*d*]thiazole (**5**; 0.094 g, 0.2 mmol, 1.0 equiv.) and *N*-iodosuccinimide (0.111 g, 0.99 mmol, 5.0 equiv.), followed by anhydrous $CHCl_3$ (0.5 mL) and glacial acetic acid (2.0 equiv.). The reaction mixture was heated at 40 °C and stirred overnight. After cooling to room temperature, the solvents were removed under reduced pressure and the residue was purified by flash column chromatography (SiO_2; PE/toluene, 3:1 to 1:1) to afford **6** as a yellow solid (0.115 g, 0.16 mmol, 80%), m.p. 131–

 © 2013 Wiley-VCH Verlag GmbH & Co. KGaA, Weinheim

133 °C. ^{1}H NMR (300 MHz, $CDCl_3$): δ = 7.17 (s, 2 H), 2.54 (t, J = 7.5 Hz, 4 H), 1.52–1.71 (m, 4 H), 1.28–1.44 (m, 12 H), 0.84–0.97 (m, 6 H) ppm. ^{13}C NMR (75 MHz, $CDCl_3$): δ = 161.9, 150.0, 148.7, 141.9, 126.9, 79.4, 32.5, 31.7, 30.0, 29.0, 22.7, 14.2 ppm. IR (KBr): $\tilde{\nu}$ = 2950, 2918, 2847, 1653, 1550, 1473, 1459, 1395, 1369, 1347, 1308, 1248, 1233, 1199, 1172, 1115, 1084 cm^{-1}. ESI-MS: m/z = 727.17 $[M + 1]^+$.

2-{4-Hexyl-5-[4-(diphenylamino)phen-1-yl]thiophen-2-yl}-5-(4-hexyl-5-iodothiophen-2-yl)thiazolo[5,4-*d*]thiazole (9a): In a Schlenk tube equipped with a magnetic stirrer were placed $[Pd(PPh_3)_4]$ (18 mg, 0.015 mmol, 0.1 equiv.) and 2,5-bis(4-hexyl-5-iodothiophen-2-yl) thiazolo[5,4-*d*]thiazole (**6**; 112 mg, 0.15 mmol, 1.0 equiv.), which were dissolved in toluene (3.0 mL). 4-(Diphenylamino)benzeneboronic acid (**7**; 45 mg, 0.15 mmol, 1.0 equiv.) was then added, followed by Na_2CO_3 (2.0 M aqueous solution, 0.39 mL, 0.77 mmol, 5.0 equiv.). The resulting mixture was heated at 90 °C and stirred for 5 h, during which the progress of the reaction was monitored by TLC (SiO_2; PE/toluene, 2:1). The reaction mixture was allowed to cool to room temperature, then diluted with H_2O (5 mL), and CH_2Cl_2 (5 mL) and stirred for 5 min. The phases were separated, and the aqueous layer was washed with CH_2Cl_2 (3× 5 mL). The combined organic layers were washed with water (10 mL) and brine (10 mL), and dried with Na_2SO_4. After filtration and evaporation of the solvent, a dark-red oil was obtained, which was purified by flash column chromatography (SiO_2; PE/toluene, 2:1) to give triarylamine **9a** (37 mg, 0.044 mmol, 28% yield) as an orange oil. ^{1}H NMR (300 MHz, $CDCl_3$): δ = 7.43 (s, 1 H), 7.26–7.34 (m, 6 H), 7.13–7.21 (m, 5 H), 7.05–7.12 (m, 4 H), 2.68 (t, J = 7.5 Hz, 2 H), 2.55 (t, J = 7.5 Hz, 2 H), 1.57–1.62 (m, 4 H), 1.22–1.45 (m, 12 H), 0.82–0.98 (m, 6 H) ppm. ^{13}C NMR (75 MHz, $CDCl_3$): δ = 163.2, 161.3, 150.0, 148.7, 147.9, 147.5, 142.0, 139.6, 138.5, 134.4, 129.9, 129.7, 129.6, 127.6, 127.2, 126.7, 125.1, 123.6, 122.7, 79.1, 32.5, 31.7 (×2), 31.0, 30.0, 29.3, 29.0 (×2), 22.7 (×2), 14.2 (×2) ppm. IR (neat): $\tilde{\nu}$ = 3059, 3035, 2954, 2925, 2854, 1733, 1645, 1593, 1552, 1479, 1328, 1315, 1280, 1192, 1178, 1116, 1093, 1075 cm^{-1}. ESI-MS: m/z = 844.32 $[M + 1]^+$.

2-{4-Hexyl-5-[4-(diphenylamino)phen-1-yl]thiophen-2-yl}-5-[4-hexyl-5-(5-formylthiophen-2-yl)thiophen-2-yl]thiazolo[5,4-*d*]thiazole (11a): In a microwave vial equipped with a magnetic stirrer were introduced compound **9a** (22 mg, 0.026 mmol, 1.0 equiv.) and $PdCl_2(dppf)\cdot CH_2Cl_2$ (ca. 2.0 mg, 2.6 μmol, 0.1 equiv.), which were dissolved in anhydrous toluene (1.0 mL). Meanwhile, into a Schlenk flask under inert atmosphere were placed 5-formyl-2-thiophenboronic acid (**10**; 12 mg, 0.078 mmol, 3.0 equiv.) and KF (9 mg, 0.16 mmol, 6.0 equiv.), which were dissolved in MeOH (1.0 equiv.). The resulting pink solution was transferred into the microwave vial, and the reaction mixture was heated under microwave irradiation at 70 °C for 20 min. The progress of the reaction was monitored by TLC (SiO_2; PE/EtOAc, 10:1), which showed that the starting material had been completely consumed. After cooling to room temperature, the reaction mixture was diluted with water (5 mL) and CH_2Cl_2 (5 mL), the layers were separated and the aqueous layer was extracted with CH_2Cl_2 (2× 5 mL). The combined organic layers were washed with brine (15 mL) and dried with Na_2SO_4. Removal of the solvent in vacuo yielded a dark-red oil, which was purified by flash column chromatography (SiO_2; PE/EtOAc, 10:1 to 5:1) to give the desired product **11a** (16 mg, 0.019 mmol, 74%) as a red oil. ^{1}H NMR (300 MHz, $CDCl_3$): δ = 9.89 (s, 1 H), 7.71 (d, J = 4.0 Hz, 1 H), 7.43 (s, 1 H), 7.38 (s, 1 H), 7.20–7.35 (m, 7 H), 7.02–7.19 (m, 8 H), 2.81 (t, J = 7.8 Hz, 2 H), 2.67 (t, J = 7.8 Hz, 2 H), 1.55–1.78 (m, 4 H), 1.19–1.50 (m, 12 H), 0.81–0.97 (m, 6 H) ppm. ^{13}C NMR (75 MHz, $CDCl_3$): δ = 182.8, 163.5, 161.0, 150.5, 150.0, 147.9, 147.4, 145.3, 143.1, 143.0, 142.2, 139.6, 137.0, 136.9, 134.2, 132.6, 129.9, 129.8, 129.6, 127.1, 126.9, 125.1, 123.7, 122.6, 31.8 (×2), 31.0, 30.3, 30.1, 29.4, 29.3, 29.1, 22.8 (×2), 14.3 (×2) ppm. IR (neat): $\tilde{\nu}$ = 3050, 2951, 2922, 2852, 1667, 1591, 1547, 1511, 1487, 1467, 1436, 1333, 1286, 1266, 1224, 1062 cm^{-1}. ESI-MS: m/z = 827.55 $[M]^+$.

2-Cyano-3-{5-[4-hexyl-2-(5-{4-hexyl-5-[4-(diphenylamino)phen-1-yl]-thiophen-2-yl}thiazolo[5,4-*d*]thiazol-2-yl)thiophen-5-yl]thiophen-2-yl}prop-2-enoic Acid (TTZ1): In a Schlenk flask equipped with a magnetic stirrer were placed aldehyde **11a** (16 mg, 0.019 mmol, 1.0 equiv.), cyanoacetic acid (7 mg, 0.077 mmol, 4.0 equiv.), ammonium acetate (2 mg, 0.025 mmol, 1.3 equiv.) and glacial acetic acid (1.5 mL). The reaction mixture was heated to 110 °C and stirred for 24 h; at this point, TLC analysis (SiO_2; PE/EtOAc, 2:1) showed the disappearance of the starting material. The reaction mixture was cooled to room temperature, water (6 mL) was added and stirring was continued for 20 min. A precipitate formed, which was collected by vacuum filtration and washed with small portions of water and methanol. The crude product was purified by crystallization from toluene followed by washing with pentane, to afford acid **TTZ1** (11 mg, 0.012 mmol, 65%) as a dark amorphous solid. ^{1}H NMR (300 MHz, $[D_8]$THF): δ = 8.37 (s, 1 H), 7.87 (d, J = 4.1 Hz, 1 H), 7.62 (s, 1 H), 7.60 (s, 1 H), 7.43 (d, J = 4.1 Hz, 1 H), 7.37 (s, 1 H), 7.35 (s, 1 H), 7.21–7.30 (m, 4 H), 7.00–7.15 (m, 8 H), 2.91 (t, J = 7.8 Hz, 2 H), 2.70 (t, J = 7.8 Hz, 2 H), 1.63–1.81 (m, 2 H), 1.45–1.54 (m, 2 H), 1.24–1.43 (m, 12 H), 0.83–0.97 (m, 6 H) ppm. ^{13}C NMR (75 MHz, $[D_8]$THF): δ = 163.7, 163.5, 161.4, 152.5, 150.6, 148.8, 148.2, 146.0, 144.9, 143.8, 142.7, 140.2, 139.0, 138.0, 137.6, 137.0, 133.5, 130.8, 130.5, 130.4, 130.1, 127.9, 127.6, 125.7, 124.2, 123.2, 116.4, 100.3, 32.4, 31.5, 31.0, 30.7, 30.1, 30.0, 29.6, 29.5, 23.3 (×2), 14.3 (×2) ppm. IR (KBr): $\tilde{\nu}$ = 3429, 3059, 3031, 2952, 2919, 2852, 2207, 1726, 1586, 1471, 1429, 1325, 1312, 1259, 1178, 1091, 1021 cm^{-1}. HRMS: m/z calcd. for $C_{50}H_{46}N_4O_2S_5$ $[M^+]$ 894.2224; found 894.2219.

Note: In the ^{1}H NMR spectra of compound TTZ1 recorded in $[D_8]$THF, the multiplet at δ = 1.63–1.81 ppm was partially or completely covered by the signal belonging to THF.

2-Cyano-3-(5-{4-hexyl-2-[5-(4-hexyl-5-{4-[bis(4-methoxyphenyl)-amino]phen-1-yl}thiophen-2-yl)thiazolo[5,4-*d*]thiazol-2-yl]thiophen-5-yl}thiophen-2-yl)prop-2-enoic Acid (TTZ2): In a Schlenk flask equipped with a magnetic stirrer were placed aldehyde **11b** (18 mg, 0.02 mmol, 1.0 equiv.), cyanoacetic acid (8 mg, 0.08 mmol, 4.0 equiv.), ammonium acetate (2 mg, 0.025 mmol, 1.3 equiv.) and glacial acetic acid (1.5 mL). The reaction mixture was heated to 110 °C and stirred for 24 h; at this point, TLC analysis (SiO_2; PE/EtOAc, 2:1) showed the disappearance of the starting material. The reaction mixture was cooled to room temperature, water (6 mL) was added and stirring was continued for 20 min. A precipitate formed, which was collected by vacuum filtration and washed with small portions of water and methanol. The crude product was purified by crystallization from toluene followed by washing with methanol and pentane, to afford acid **TTZ2** (12 mg, 0.013 mmol, 65%) as a dark amorphous solid. ^{1}H NMR (400 MHz, $[D_8]$THF): δ = 8.37 (s, 1 H), 7.87 (d, J = 3.9 Hz, 1 H), 7.62 (s, 1 H), 7.58 (s, 1 H), 7.43 (d, J = 3.9 Hz, 1 H), 7.27 (d, J = 8.5 Hz, 2 H), 7.09 (d, J = 8.5 Hz, 4 H), 6.83–6.94 (m, 6 H), 3.77 (s, 6 H), 2.91 (t, J = 7.8 Hz, 2 H), 2.69 (t, J = 7.8 Hz, 2 H), 1.63–1.81 (m, 2 H), 1.43–1.55 (m, 2 H), 1.22–1.41 (m, 12 H), 0.82–0.96 (m, 6 H) ppm. ^{13}C NMR (100 MHz, $[D_8]$THF): δ = 163.69, 163.65, 161.3, 157.6, 151.2, 150.6, 149.8, 146.0, 144.9, 143.8, 143.4, 141.0, 139.8, 138.9, 137.7, 137.0, 134.8, 133.4, 130.8, 130.5, 130.1, 127.9, 127.6, 125.5, 119.7, 116.4, 115.4, 100.3, 55.4, 32.4, 31.5, 31.0, 30.6, 30.5, 30.0, 29.9, 29.5, 23.3 (×2), 14.2 (×2) ppm. IR (KBr): $\tilde{\nu}$ = 3444, 2957, 2852,

 © 2013 Wiley-VCH Verlag GmbH & Co. KGaA, Weinheim

2210, 1651, 1505, 1318, 1260, 1242, 1093, 1035 cm^{-1}. HRMS: *m*/*z* calcd. for $C_{52}H_{50}N_4O_4S_5$ $[M]^+$ 954.2436; found 954.2428.

Note: In the ^{1}H-NMR spectra of compound TTZ2 recorded in [D_8]THF, the multiplet at δ = 1.63–1.81 ppm was partially or completely covered by the signal belonging to THF.

2-Cyano-3-{5-[4-hexyl-2-(5-{4-hexyl-6-[4-(diphenylamino)phen-1-yl]-thiophen-2-yl}benzobis(1,2-*d*;4,5-*d*′)thiazol-2-yl)thiophen-5-yl]thiophen-2-yl}prop-2-enoic Acid (BBZ1): Into a Schlenk flask equipped with a magnetic stirrer was placed aldehyde **16a** (38 mg, 0.043 mmol, 1.0 equiv.). Cyanoacetic acid (73 mg, 0.86 mmol) and ammonium acetate (22 mg, 0.28 mmol) were dissolved in glacial acetic acid (7.5 mL) at room temperature and an aliquot (1.5 mL) of the resulting solution was then added to the substrate, corresponding to the following quantities: cyanoacetic acid (14.6 mg, 0.17 mmol, 4.0 equiv.), ammonium acetate (4.3 mg, 0.056 mmol, 1.3 equiv.). The reaction mixture was heated to reflux and stirred for 48 h, after which it was allowed to cool to room temperature. The reaction mixture was poured into water (ca. 10 mL) and the resulting precipitate was filtered off, washed with water and dried. Recrystallization from toluene, followed by washing with methanol and pentane afforded carboxylic acid **BBZ1** (15 mg, 0.016 mmol, 37%) as a dark-red amorphous solid. ^{1}H NMR (400 MHz, [D_8]THF): δ = 8.47 (s, 1 H), 8.46 (s, 1 H), 8.38 (s, 1 H), 7.88 (d, *J* = 4.0 Hz, 1 H), 7.67 (s, 1 H), 7.65 (s, 1 H), 7.47 (d, *J* = 4.0 Hz, 1 H), 7.39 (d, *J* = 8.6 Hz, 2 H), 7.25–7.31 (m, 4 H), 7.02–7.16 (m, 8 H), 2.92 (t, *J* = 7.9 Hz, 2 H), 2.73 (t, *J* = 7.8 Hz, 2 H), 1.70–1.78 (m, 4 H), 1.30–1.42 (m, 12 H), 0.86–0.94 (m, 6 H) ppm. ^{13}C NMR (100 MHz, [D_8]THF): δ = 163.8, 162.6, 161.2, 153.1, 152.6, 148.8, 148.2, 145.9, 144.8, 143.75, 143.68, 140.2, 138.9, 137.4, 137.2, 135.4, 135.3, 135.1, 134.5, 132.9, 132.4, 130.4, 130.1, 128.5, 128.0, 127.8, 125.7, 124.2, 123.2, 116.4, 115.9, 115.6, 32.4, 31.5, 31.1, 30.6, 30.5, 30.0, 29.9, 29.5, 23.3 (×2), 14.3 (×2) ppm. IR (KBr): $\tilde{\nu}$ = 3434, 2961, 2924, 2852, 2206, 1729, 1580, 1489, 1432, 1310, 1261, 1087, 1020 cm^{-1}. HRMS: *m*/*z* calcd. for $C_{54}H_{48}N_4O_2S_5$ $[M + 1]^+$ 945.2454; found 945.2451.

Note: In the ^{1}H-NMR spectra of compound BBZ1 recorded in [D_8]THF, the multiplet at δ = 1.70–1.78 ppm was partially or completely covered by the signal belonging to THF.

2-Cyano-3-(5-{4-hexyl-2-[5-(4-hexyl-6-{4-[bis(4-methoxyphenyl)-amino]phen-1-yl}thiophen-2-yl)benzobis(1,2-*d*;4,5-*d*′)thiazol-2-yl]-thiophen-5-yl}thiophen-2-yl)prop-2-enoic Acid (BBZ2): Into a Schlenk flask equipped with a magnetic stirrer was placed aldehyde **16b** (25 mg, 0.027 mmol, 1.0 equiv.), which was dissolved in glacial acetic acid (2.0 mL) at room temperature. Cyanoacetic acid (30 mg, 0.35 mmol, 13.0 equiv.) was added, followed by ammonium acetate (50 mg, 0.4 mmol, 14.4 equiv.). The reaction mixture was heated to reflux and stirred for 48 h, after which it was allowed to cool to room temperature. The reaction mixture was poured into water (ca. 10 mL) and the resulting precipitate was filtered off, washed with water and dried. Recrystallization from toluene, followed by washing with a large volume of methanol and pentane afforded carboxylic acid **BBZ2** (10 mg, 0.01 mmol, 37%) as a dark-red amorphous solid. ^{1}H NMR (300 MHz, [D_8]THF): δ = 8.48 (s, 1 H), 8.46 (s, 1 H), 8.39 (s, 1 H), 7.89 (d, *J* = 4.0 Hz, 1 H), 7.68 (s, 1 H), 7.64 (s, 1 H), 7.48 (d, *J* = 4.0 Hz, 1 H), 7.30 (d, *J* = 8.7 Hz, 2 H), 7.05–7.14 (m, 4 H), 6.83–6.95 (m, 6 H), 3.77 (s, 6 H), 2.93 (t, *J* = 7.8 Hz, 2 H), 2.71 (t, *J* = 7.8 Hz, 2 H), 1.72–1.78 (m, 2 H), 1.48–1.54 (m, 2 H), 1.23–1.45 (m, 12 H), 0.83–0.97 (m, 6 H) ppm. ^{13}C NMR (100 MHz, [D_8]THF): δ = 163.7, 162.6, 161.1, 157.6, 153.2, 152.5, 149.9, 146.0, 144.9, 144.3, 143.8, 141.0, 139.8, 138.9, 137.4, 137.2, 135.4, 135.2, 134.6, 134.5, 132.9, 132.4, 130.2, 127.9, 125.6, 119.7, 116.4, 115.8, 115.5, 115.4, 111.4, 100.5, 55.4, 32.44, 32.42, 31.6, 31.1, 30.6, 30.01, 29.95, 29.5, 23.3 (×2), 14.2 (×2) ppm. IR (KBr): $\tilde{\nu}$ = 3418, 2951, 2925, 2854, 2208, 1584, 1505, 1495, 1435, 1312, 1241, 1192, 1059, 1036 cm^{-1}. HRMS: *m*/*z* calcd. for $C_{56}H_{52}N_4O_4S_5$ $[M]^+$ 1004.2587; found 1004.2596.

Note: In the ^{1}H-NMR spectra of compound BBZ2 recorded in [D_8]THF, the multiplet at δ = 1.72–1.78 ppm was partially or completely covered by the signal belonging to THF.

Cyclic Voltammetry and Spectroelectrochemical Measurements: Anhydrous 99.9%, HPLC grade dichloromethane for electrochemistry was purchased from Aldrich. The supporting electrolyte used was electrochemical grade $[N(Bu)_4]PF_6$ obtained from Fluka. Cyclic voltammetry was performed in a three-electrode C-3 BAS Cell having a platinum working electrode, a platinum counter electrode and an aqueous Ag/AgCl NaCl (3 M) reference electrode. A BAS 100A electrochemical analyser was used as a polarizing unit. Under these experimental conditions, the one-electron oxidation of ferrocene occurs at $E°'$ = +0.42 V. UV/Vis spectroelectrochemical measurements were carried out with a Perkin–Elmer Lambda 2 UV/Vis spectrophotometer and a Optically Transparent Thin Layer spectroelectrochemical (OTTLE) cell in quartz glass with an optical path-length of 1 mm, equipped with a Pt-minigrid working electrode, a Pt auxiliary electrode and an Ag/AgCl NaCl (3 M) reference electrode. A nitrogen-saturated CH_2Cl_2 solution of the compound under study was used with $[N(Bu)_4][PF_6]$ (0.2 M) as the supporting electrolyte. The in situ spectroelectrochemistry was recorded by collecting spectra in the spectral window 250–1000 nm during the stepwise oxidation of the compound (*Ei* = +0.55 V, ΔE = 50 mV, Δt = 1 min). A BAS 100A electrochemical analyzer was used as the polarizing unit during all the experiments.

Computational Details: DFT calculations were performed with the Gaussian09 program package.[38] Geometry optimizations were carried out in vacuo using the B3LYP functional[45] and the standard 6-31G* basis set for all atoms. The absorption maxima (λ^a_{max}), vertical excitation energies (E_{exc}) and oscillator strengths (*f*) were calculated, both in vacuo and in THF, on the optimized structure by time-dependent DFT (TD-DFT) at the CAM-B3LYP/6-31G* level.[46] Solvent effects were included by using the polarizable continuum model (PCM).[47]

DSSC Fabrication and Photoelectrochemical Measurements: FTO-coated conducting glass (TCO 30–8, Solaronix) was cut into 20 × 20 mm slides by using a diamond point. The slides were cleaned by immersing them in ethanol for 15 min and, subsequently, in acetone for 15 min using an ultrasound bath, followed by rinsing with water and ethanol. The slides were then immersed in a 0.04 M $TiCl_4$ aqueous solution at 70 °C for 30 min, followed by rinsing with water and ethanol. A commercially available nanocrystalline TiO_2 paste (Ti-Nanoxide D/SP, Solaronix) was printed on the cleaned FTO glass by means of squeegee printing. The active area of the resulting nanocrystalline TiO_2 films was 0.25 cm^2. The films were kept in a clean box for 5 min with ethanol so that the film could relax, and were then heated on a hot plate at 125 °C for 15 min to remove any trace of water. Subsequently, they were sintered for 30 min at 280 °C, followed by 30 min at 450 °C. The coated glass slides were again immersed in a 0.04 M $TiCl_4$ aqueous solution at 70 °C for 30 min, followed by rinsing with water and ethanol. Finally, they were sintered at 450 °C for 30 min and allowed to cool under air until they reached a temperature of 70 °C. At this point, the electrodes were immersed in a 5×10^{-4} M solution of the appropriate dye in THF for at least 10 h; in the case of measurements performed in the presence of a co-adsorbent, the solution contained also chenodeoxycholic acid (CDCA) in a 2.5×10^{-3} M concentration. Once the staining procedure was com-

 © 2013 Wiley-VCH Verlag GmbH & Co. KGaA, Weinheim

plete, the electrodes were rinsed with ethanol and dried under a flow of air. For the preparation of the counter electrodes, the FTO conducting glass was cut and the resulting slides were cleaned as described above; a small hole (approx. 1 mm diameter) was then drilled on every slide by using a diamond-point drill. A commercial platinum-based paint (Platisol T, Solaronix) was deposed on the conductive side of the FTO-coated glass by using a brush, followed by drying at 125 °C for 15 min and sintering at 400 °C for 30 min. The two electrodes were assembled into a sandwich type cell by heating at 250 °C with a hot-melt ionomer film (Meltonix 1170-25, Solaronix) as a spacer between them. A drop of the appropriate electrolyte solution was placed on the drilled hole on the back of the counter electrode and was driven into the cell by vacuum backfilling. The hole was finally sealed by using additional sealing film and a small glass cover (0.1 cm^2).

The iodine-based electrolyte solution was composed of 0.6 M 1-butyl-3-mehtylimidazolium iodide, 0.025 M lithium iodide, 0.04 M iodine, 0.28 M *tert*-butylpyridine and 0.05 M guanidinium isocyanate in an 85:15 mixture of acetonitrile and valeronitrile.

The photoelectrochemical characterization of the solar cells was performed by using a Abet Technologies Sun 2000 class AAA solar simulator under global AM 1.5 sunlight. The power of the incoming radiation was set to 90 $mW\,cm^{-2}$ by means of a Kipp & Zonen CMP3 pyranometer. *J*/*V* curves were obtained with a Keithley 220 programmable power source coupled with a Keithley 181 nanovoltmeter, under the control of software developed in-house.

Electrochemical impedance spectroscopy (EIS) was performed in the dark by using a Parstat 2273 potentiostat, with a –0.60 V forward bias. The spectra were recorded over a frequency range of 0.1 Hz to 10^5 Hz with an amplitude of 10 mV.

Measurement of the Density of Adsorbed Dyes on TiO_2: A nanocrystalline TiO_2 electrode (surface area 0.88 cm^2) similar to those used for the photovoltaic measurements (see previous section) was immersed in 4.5×10^{-4} M solutions of either dye **TTZ2** or **BBZ2** in THF at room temp. for 16 h. The stained electrode was removed from the solution, dried under a stream of nitrogen and immersed in 5 mL of a 0.2 M KOH solution in THF/MeOH (9:1) at room temp. until full decoloration was observed. The absorbance of the resulting orange-yellow solution was measured by UV/Vis spectroscopy and compared to that of a standard 3.0×10^{-5} M solution of sensitizer in the same solvent/base mixture. The amount of dye present in the unknown solution was calculated and divided by the electrode surface area, yielding density values of approx. 4.0×10^{-7} and 2.9×10^{-7} $mol\,cm^{-2}$ for compounds **TTZ2** and **BBZ2**, respectively.

Supporting Information (see footnote on the first page of this article): Complete experimental procedures for the synthesis of compounds **3**, **8**, **9b**, **11b**, **13**, **14**, **15a**–**b** and **16a**–**b**, copies of ^1H and ^{13}C NMR spectra of compounds **TTZ1**–**2** and **BBZ1**–**2**, additional computational, spectroscopic and electrochemical data.

Acknowledgments

M. L. P. and M. C. are grateful to Regione Toscana within the POR-FSE 2007-2013 program for a postdoctoral fellowship (FOTOSENSORG project). Dr. Jonathan Filippi (ICCOM-CNR) is gratefully acknowledged for his help in performing EIS measurements. A. S., M. L. P. and R. B. acknowledge CINECA awards N. HP10C9HMGL and N. HP10CJ65S2, 2011 for the availability of high performance computing resources and support.

[1] See, for example: *BP Statistical Review of World Energy 2012*, available at: www.bp.com/statisticalreview.
[2] See, for example: a) V. Balzani, N. Armaroli, *Energy for a Sustainable World*, Wiley-VCH, Weinheim, Germany, **2010**; b) J. Twidell, T. Weir, *Renewable Energy Resources*, Taylor & Francis, Oxon, United Kingdom, **2006**.
[3] Q. Schiermeier, J. Tollefson, T. Scully, A. Witze, O. Morton, *Nature* **2008**, *454*, 816.
[4] T. Saga, *NPG Asia Mater.* **2010**, *2*, 96.
[5] B. O'Reagan, M. Grätzel, *Nature* **1991**, *353*, 737.
[6] A. Hagfeldt, G. Boschloo, L. Sun, L. Kloo, H. Pettersson, *Chem. Rev.* **2010**, *110*, 6595.
[7] See, for example: a) M. K. Nazeeruddin, A. Kay, I. Rodicio, R. Humphry-Baker, E. Mueller, P. Liska, N. Vlachopoulos, M. Grätzel, *J. Am. Chem. Soc.* **1993**, *115*, 6382; b) M. K. Nazeeruddin, P. Pechy, M. Grätzel, *Chem. Commun.* **1997**, 1705; c) M. K. Nazeeruddin, P. Pechy, T. Renouard, S. M. Zakeeruddin, R. Humphry-Baker, P. Comte, P. Liska, L. Cevey, E. Costa, V. Shklover, L. Spiccia, G. B. Deacon, C. A. Bignozzi, M. Grätzel, *J. Am. Chem. Soc.* **2001**, *123*, 1613.
[8] C.-Y. Chen, M. Wang, J.-Y. Li, N. Pootrakulchote, L. Alibabaei, C.-H. Ngoc-le, J.-D. Decoppet, J.-H. Tsai, C. Grätzel, C.-G. Wu, S. M. Zakeeruddin, M. Grätzel, *ACS Nano* **2010**, *3*, 3103.
[9] a) Y. Ooyama, Y. Harima, *Eur. J. Org. Chem.* **2009**, 2903; b) A. Mishra, M. K. R. Fischer, P. Bäuerle, *Angew. Chem.* **2009**, *121*, 2510; *Angew. Chem. Int. Ed.* **2009**, *48*, 2474.
[10] A CAS SciFinder search using the keywords "organic dyes" and "dye-sensitized solar cell" yielded 242 results for the year 2010 and 320 results for the year 2011.
[11] J. Ephraim, *Ber. Dtsch. Chem. Ges.* **1891**, *24*, 1026.
[12] J. R. Johnson, R. Ketcham, *J. Am. Chem. Soc.* **1960**, *82*, 2719.
[13] J. R. Johnson, D. H. Rotenberg, R. Ketcham, *J. Am. Chem. Soc.* **1970**, *92*, 4046.
[14] a) R. Ketcham, S. Mah, *J. Med. Chem.* **1971**, *14*, 743; b) R. B. Moffett, *J. Heterocycl. Chem.* **1980**, *17*, 753.
[15] I. H. Jung, Y. K. Jung, J. Lee, J.-H. Park, H. Y. Woo, J.-I. Lee, H. Y. Chu, H.-K. Shim, *J. Polym. Sci., Part A: Polym. Chem.* **2008**, *46*, 7148.
[16] a) S. Ando, J.-i. Nishida, H. Tada, Y. Inoue, S. Tokito, Y. Yamashita, *J. Am. Chem. Soc.* **2005**, *127*, 5336; b) M. Mamada, J.-i. Nishida, D. Kumaki, S. Tokito, Y. Yamashita, *Chem. Mater.* **2007**, *19*, 5404; c) I. Osaka, G. Sauvé, R. Zhang, T. Kowalewski, R. D. McCullough, *Adv. Mater.* **2007**, *19*, 4160; d) I. Osaka, R. Zhang, G. Sauvé, D.-M. Smilgies, T. Kowalewski, R. D. McCullough, *J. Am. Chem. Soc.* **2009**, *131*, 2521; e) I. Osaka, R. Zhang, J. Liu, D.-M. Smilgies, T. Kowalewski, R. D. McCullough, *Chem. Mater.* **2010**, *22*, 4191.
[17] a) I. H. Jung, J. Yu, E. Jeong, J. Kim, S. Kwon, H. Kong, K. Lee, H. Y. Woo, H.-K. Shim, *Chem. Eur. J.* **2010**, *16*, 3743; b) Q. Shi, H. Fan, Y. Liu, W. Hu, Y. Li, X. Zhan, *J. Phys. Chem. C* **2010**, *114*, 16843; c) M. Yang, B. Peng, B. Liu, Y. Zou, K. Zhou, Y. He, C. Pan, Y. Li, *J. Phys. Chem. C* **2010**, *114*, 17989; d) S. K. Lee, J. M. Cho, Y. Goo, W. S. Shin, J.-C. Lee, W.-H. Lee, I.-N. Kang, H.-K. Shim, S.-J. Moon, *Chem. Commun.* **2011**, *47*, 1791; e) J. Peet, L. Wen, P. Byrne, S. Rodman, K. Forberich, Y. Shao, N. Drolet, R. Gaudiana, G. Dennler, D. Waller, *Appl. Phys. Lett.* **2011**, *98*, 043301; f) M. Zhang, X. Guo, Y. Li, *Adv. Energy Mater.* **2011**, *1*, 557; g) S. Subramaniyan, H. Xin, F. S. Kim, S. Shoaee, J. R. Durrant, S. A. Jenekhe, *Adv. Energy Mater.* **2011**, *1*, 854; h) T. M. Clarke, D. Rodovsky, A. A. Herzing, J. Peet, G. Dennler, D. DeLongchamp, C. Lungenschmied, A. J. Mozer, *Adv. Energy Mater.* **2011**, *1*, 1062; i) L. Huo, X. Guo, S. Zhang, Y. Li, J. Hou, *Macromolecules* **2011**, *44*, 4035; j) S. Subramanyian, H. Xin, F. S. Kim, S. Jenekhe, *Macromolecules* **2011**, *44*, 6245; k) T. M. Clarke, J. Peet, P. Denk, G. Dennler, C. Lungenschmied, A. J. Mozer, *Energy Environ. Sci.* **2012**, *5*, 5241; l) P. Dutta, W. Yang, S. H. Eom, S.-H. Lee, *Org. Electron.* **2012**, *13*, 273.

 © 2013 Wiley-VCH Verlag GmbH & Co. KGaA, Weinheim

[18] M. Zhang, X. Guo, X. Wang, H. Wang, Y. Li, *Chem. Mater.* **2011**, *23*, 4264.
[19] A. G. Green, A. G. Perkin, *J. Chem. Soc.* **1903**, *83*, 1201.
[20] a) A. I. Kiprianov, F. A. Mikhailenko, *Chem. Heterocycl. Compd.* **1967**, *3*, 205; b) J. K. Landquist, *J. Chem. Soc. C* **1967**, 2212; c) G. Grandolini, A. Martani, A. Ricci, N. Cagnoli-Bellavita, *Ann. Chim.* **1968**, *58*, 91; d) S. L. Solar, R. J. Cox, N. J. Clecak, R. Ettinger, *J. Org. Chem.* **1968**, *33*, 2132.
[21] a) A. I. Kiprianov, F. A. Mikhailenko, I. L. Mushkalo, *Chem. Heterocycl. Compd.* **1970**, *6*, 1340; b) J. F. Mike, J. J. Interman, A. Ellern, M. Jeffries-EL, *J. Org. Chem.* **2010**, *75*, 495.
[22] a) J. A. Osaheni, S. A. Jenekhe, *Chem. Mater.* **1992**, *4*, 1282; b) J. A. Osaheni, S. A. Jenekhe, *Chem. Mater.* **1995**, *7*, 672; c) S.-H. Lee, A. Otomo, T. Nakahama, T. Yamada, T. Kamikado, S. Yokohama, S. Mashiko, *J. Mater. Chem.* **2002**, *12*, 2187.
[23] a) M. M. Alam, S. A. Jenekhe, *Chem. Mater.* **2002**, *14*, 4775; b) H. Pang, F. Vilela, P. J. Skabara, J. J. W. McDouall, D. J. Crouch, T. D. Anthopoulos, D. D. C. Bradley, D. M. de Leeuw, P. H. Horton, M. B. Hursthouse, *Adv. Mater.* **2007**, *19*, 4438; c) I. Osaka, K. Takimiya, R. D. McCullough, *Adv. Mater.* **2010**, *22*, 4993.
[24] S. Yao, H.-Y. Ahn, X. Wang, J. Fu, E. W. Van Stryland, D. J. Hagan, K. D. Belfield, *J. Org. Chem.* **2010**, *75*, 3965.
[25] G. M. Fischer, E. Daltrozzo, A. Zumbusch, *Angew. Chem.* **2011**, *123*, 1442; *Angew. Chem. Int. Ed.* **2011**, *50*, 1406.
[26] H.-H. G. Tsai, L.-C. Chou, S.-C. Lin, H.-S. Sheu, C. K. Lai, *Tetrahedron Lett.* **2009**, *50*, 1906.
[27] a) E. Ahmed, F. S. Kim, H. Xin, S. A. Jenekhe, *Macromolecules* **2009**, *42*, 8615; b) E. Ahmed, S. Subramaniyan, F. S. Kim, H. Xin, S. A. Jenekhe, *Macromolecules* **2011**, *44*, 7207.
[28] N. Koumura, Z.-S. Wang, S. Mori, M. Miyashita, E. Suzuki, K. Hara, *J. Am. Chem. Soc.* **2006**, *128*, 14256.
[29] a) J. A. Zampese, F. R. Keeneb, P. J. Steel, *Dalton Trans.* **2004**, 4124; b) J. W. Slater, P. J. Steel, *Tetrahedron Lett.* **2006**, *47*, 6941; c) R. C. Knighton, A. J. Hallett, B. M. Kariuki, S. J. A. Pope, *Tetrahedron Lett.* **2010**, *51*, 5419; d) D. Li, Y. Yuan, H. Bi, D. Yao, X. Zhao, W. Tian, Y. Wang, H. Zhang, *Inorg. Chem.* **2011**, *50*, 4825; e) J. Y. Jung, S. J. Han, J. Chun, C. Lee, J. Yoon, *Dyes Pigm.* **2012**, *94*, 423.
[30] C. Lambert, J. Schelter, T. Fiebig, D. Mank, A. Trifonov, *J. Am. Chem. Soc.* **2005**, *127*, 10600.
[31] a) K. R. J. Thomas, J. T. Lin, Y.-C. Hsu, K.-C. Ho, *Chem. Commun.* **2008**, 4098; b) M. S. Tsai, Y.-C. Hsu, J. T. Lin, H.-C. Chen, C.-P. Hsu, *J. Phys. Chem. C* **2007**, *111*, 18785; c) J. Jia, K. Cao, P. Xue, Y. Zhang, H. Zhou, R. Lu, *Tetrahedron* **2012**, *68*, 3626.
[32] a) J. Song, F. Zhang, C. Li, W. Liu, B. Li, Y. Huang, Z. Bo, *J. Phys. Chem. C* **2009**, *113*, 13391; b) W. Wu, J. Yang, J. Hua, J. Tang, L. Zhang, Y. Long, H. Tian, *J. Mater. Chem.* **2010**, *20*, 1772; c) Y. Numata, I. Ashraful, Y. Shirai, L. Han, *Chem. Commun.* **2011**, *47*, 6159.
[33] a) D. P. Hagberg, T. Edvinsson, T. Marinado, G. Boschloo, A. Hagfeldt, L. Sun, *Chem. Commun.* **2006**, 2245; b) D. P. Hagberg, T. Marinado, K. M. Karlsson, K. Nonomura, P. Qin, G. Boschloo, T. Brinck, A. Hagfeldt, L. Sun, *J. Org. Chem.* **2007**, *72*, 9550.
[34] a) S.-L. Li, K.-J. Jiang, K.-F. Shao, L.-M. Yang, *Chem. Commun.* **2006**, 2792; b) Y. Liang, B. Peng, J. Liang, Z. Tao, J. Chen, *Org. Lett.* **2010**, *12*, 1204.
[35] a) A. C. Benniston, A. Harriman, D. J. Lawrie, A. Mayeux, *Phys. Chem. Chem. Phys.* **2004**, *6*, 51; b) J. T. Lin, P.-C. Chen, Y.-S. Yen, Y.-C. Hsu, H.-H. Chou, M.-C. P. Yeh, *Org. Lett.* **2009**, *11*, 97; c) H. Zhou, P. Xue, Y. Zhang, X. Zhao, J. Jia, X. Zhang, X. Liu, R. Lu, *Tetrahedron* **2011**, *67*, 8477.
[36] S. Dapperheld, E. Steckhan, K. H. Grosse Brinkhaus, T. Esch, *Chem. Ber.* **1991**, *124*, 2557.
[37] C. Lambert, G. Nöll, *J. Am. Chem. Soc.* **1999**, *121*, 8434.
[38] M. J. Frisch, G. W. Trucks, H. B. Schlegel, G. E. Scuseria, M. A. Robb, J. R. Cheeseman, G. Scalmani, V. Barone, B. Mennucci, G. A. Petersson, H. Nakatsuji, M. Caricato, X. Li, H. P. Hratchian, A. F. Izmaylov, J. Bloino, G. Zheng, J. L. Sonnenberg, M. Hada, M. Ehara, K. Toyota, R. Fukuda, J. Hasegawa, M. Ishida, T. Nakajima, Y. Honda, O. Kitao, H. Nakai, T. Vreven, J. A. Montgomery, Jr., J. E. Peralta, F. Ogliaro, M. Bearpark, J. J. Heyd, E. Brothers, K. N. Kudin, V. N. Staroverov, R. Kobayashi, J. Normand, K. Raghavachari, A. Rendell, J. C. Burant, S. S. Iyengar, J. Tomasi, M. Cossi, N. Rega, J. M. Millam, M. Klene, J. E. Knox, J. B. Cross, V. Bakken, C. Adamo, J. Jaramillo, R. Gomperts, R. E. Stratmann, O. Yazyev, A. J. Austin, R. Cammi, C. Pomelli, J. W. Ochterski, R. L. Martin, K. Morokuma, V. G. Zakrzewski, G. A. Voth, P. Salvador, J. J. Dannenberg, S. Dapprich, A. D. Daniels, Ö. Farkas, J. B. Foresman, J. V. Ortiz, J. Cioslowski, D. J. Fox, *Gaussian 09*, Revision A.1, Gaussian, Inc., Wallingford, CT, **2009**.
[39] Please note that in Figure 7 the I^-/I_3^- redox potential seems to be comparable with HOMO energies of dyes **TTZ2** and **BBZ2**, however, it was observed that calculations on D-π-A dyes usually overestimate HOMO positions by ca. 0.6 V, see: a) D. P. Hagberg, J. H. Yum, H. J. Lee, F. De Angelis, T. Marinado, K. M. Karlsson, R. Humphry-Baker, L. Sun, A. Hagfeldt, M. Grätzel, M. K. Nazeeruddin, *J. Am. Chem. Soc.* **2008**, *130*, 6259; b) J. H. Yum, D. P. Hagberg, S. J. Moon, K. M. Karlsson, T. Marinado, L. Sun, A. Hagfeldt, M. K. Nazeeruddin, M. Grätzel, *Angew. Chem.* **2009**, *121*, 1604; *Angew. Chem. Int. Ed.* **2009**, *48*, 1576; c) S. Meng, E. Kaxiras, M. K. Nazeeruddin, M. Grätzel, *J. Phys. Chem. C* **2011**, *115*, 9276, and references cited therein.
[40] See, for example: a) A. Kay, M. Grätzel, *J. Phys. Chem.* **1993**, *97*, 6272; b) K. Hara, Y. Dan-oh, C. Kasada, Y. Ohga, A. Shinpo, S. Suga, K. Sayama, H. Arakawa, *Langmuir* **2004**, *20*, 4205; c) S. Ko, H. Choi, M.-S. Kang, H. Hwang, H. Ji, J. Kim, J. Ko, Y. Kang, *J. Mater. Chem.* **2010**, *20*, 2391; d) J. Mao, F. Guo, W. Ying, W. Wu, J. Li, J. Hua, *Chem. Asian J.* **2012**, *7*, 982.
[41] H. Tian, X. Yang, J. Cong, R. Chen, C. Teng, J. Liu, Y. Hao, L. Wang, L. Sun, *Dyes Pigm.* **2010**, *84*, 62.
[42] See, for example: a) Q. Wang, J.-E. Moser, M. Grätzel, *J. Phys. Chem. B* **2005**, *109*, 14945; b) F. Fabregat-Santiago, J. Bisquert, G. Garcia-Belmonte, G. Boschloo, A. Hagfeldt, *Sol. Energy Mater. Sol. Cells* **2005**, *87*, 117; c) F. Fabregat-Santiago, J. Bisquert, L. Cevey, P. Chen, M. Wang, S. M. Zakeeruddin, M. Grätzel, *J. Am. Chem. Soc.* **2009**, *131*, 558.
[43] W. Schlenk, E. Bergmann, *Justus Liebigs Ann. Chem.* **1928**, *22*, 464.
[44] W. C. Still, M. Kahn, A. Mitra, *J. Org. Chem.* **1978**, *43*, 2923.
[45] a) A. D. Becke, *J. Chem. Phys.* **1993**, *98*, 5648; b) C. Lee, W. Yang, R. G. Parr, *Phys. Rev. B* **1988**, *37*, 785.
[46] T. Yanai, D. Tew, N. Handy, *Chem. Phys. Lett.* **2004**, *393*, 51.
[47] J. Tomasi, B. Mennucci, R. Cammi, *Chem. Rev.* **2005**, *105*, 2999.

Received: December 3, 2012
Published Online: February 18, 2013

 © 2013 Wiley-VCH Verlag GmbH & Co. KGaA, Weinheim